Enhanced Uptake of PAHs by Organic-Coated Aqueous Surfaces

Baagi T. Mmereki, Sri R. Chaudhuri, and D. J. Donaldson*

Department of Chemistry and UTSC, University of Toronto, 80 St. George Street, Toronto, Ontario, Canada M5S 3H6

Received: October 31, 2002; In Final Form: December 30, 2002

We report direct laser-induced fluorescence measurements of the uptake of the polycyclic aromatic hydrocarbons (PAHs) anthracene and pyrene to the air−aqueous interface for pure water and for water coated with an organic film. The surface uptake coefficients of anthracene and pyrene to the air−water interface are estimated to be on the order of 10^{-5}. For both PAHs, the surface uptake coefficients for uptake to a 1-octanol-coated water surface increase by a factor of 2−3 over those determined for the pure water surface. The surface uptake of pyrene to a hexanoic-acid-coated interface does not display this enhancement, though there is a small enhancement of its equilibrium partitioning to hexanoic-acid-coated surfaces. Resolved fluorescence spectra of pyrene adsorbed onto 1-octanol-coated surfaces indicate that pyrene is in a less polar environment there than when adsorbed at hexanoic-acid-coated interfaces.

Introduction

Many important environmental processes are governed by heterogeneous interactions of gas-phase molecules with aqueous surfaces. In the troposphere, where water is abundant in all its physical phases, the partitioning of organic compounds to the air−water interface of aqueous particles such as aerosols and fog droplets may play an important role in the deposition mechanisms and reactivity of the organic compounds. The thermodynamic propensity for partitioning of organic compounds at the air−water interface has been the subject of recent work from this laboratory[1−4] and elsewhere.[5−10] Such partitioning of organic compounds to the air−water interface may promote formation of an organic film on the surface of these particles.

The possible existence of an organic film on atmospheric aerosol particles, fog droplets, cloud droplets, rain droplets, and snow flakes was first suggested by Gill and Graedel,[11] and has very recently been confirmed by field measurements of Tervahattu and co-workers.[12] Ellison et al.[13] have suggested that atmospheric oxidative processing of organic-coated aerosols might modify their chemical and radiative transfer properties. An enhanced oxidation rate of unsaturated fatty acids by ozone has been observed when the fatty acid was adsorbed to the air−water interface.[14] The presence of an organic film on atmospheric particles may have other consequences as well; for instance, it may enhance the gas−surface and solution−surface partitioning of hydrophobic compounds such as polycyclic aromatic hydrocarbons (PAHs).[15,16]

We have very recently reported an enhanced partitioning of pyrene (up to a factor of 2) from the solution phase to the air−aqueous interface, when that interface is coated with submonolayer to monolayer amounts of hexanoic acid.[17] Both the fluorescence lifetime and the resolved fluorescence spectrum of pyrene measured at the hexanoic-acid-coated water surface differ from those measured in solution. They differ as well from those measured at the surface of either pure water or pure hexanoic acid, suggesting that the coated interface represents a chemical environment that is different from that of either of the "pure" surfaces. No evidence was seen for self-association of pyrene at the interface of any of the coated or uncoated solutions. We suggested that an analogous enhanced partitioning to organic-coated aqueous surfaces might help explain the observed enrichment of hydrophobic organic compounds associated with fog water and aerosols.[18−21]

In the present report, we extend the work presented in ref 17 to measurements of the uptake kinetics of anthracene and pyrene from the gas phase to the air−aqueous interface. The gas-to-surface uptake coefficient is estimated for surfaces of pure water and of aqueous solutions of 1-octanol and of hexanoic acid. To our knowledge, this is the first direct measurement of uptake to a liquid surface.

Experimental Section

Both equilibrium and time-dependent measurements were carried out in this work. The equilibrium studies used the apparatus described in ref 17; the kinetic experiments used a modified version of that setup, illustrated in Figure 1. Several grams of PAH were placed in a container which was immersed in a water bath set to 80 °C. Prepurified N_2 flowed over the sample at a rate of (1.2 ± 0.1) L min^{-1}, as determined by a mass flow meter. The mixture of PAH and N_2 flowed through ∼ 50 cm of room temperature 1/4" tubing, before entering a side neck of a 100 mL three-necked, round-bottomed flask containing a room-temperature sample of the substrate solution. We assume that this length of tubing is sufficient to ensure that the PAH entering the sample flask is at its room temperature vapor pressure. The exhaust from the sample flask was collected from the other side neck and passed through two traps to capture any remaining PAH.

Fluorescence was collected perpendicular to the liquid surface through the central neck of the sample flask after excitation by a pulsed nitrogen laser operating at a repetition rate of 10 Hz. The laser beam impinged on the sample at an angle of ∼ 85° to the surface normal such that it made a glancing reflection at the surface of the solution. A 7 mm diameter fiber optic bundle

* Author to whom correspondence should be addressed. E-mail: jdonalds@chem.utoronto.ca.

10.1021/jp027361g CCC: $25.00
Published on Web 03/07/2003

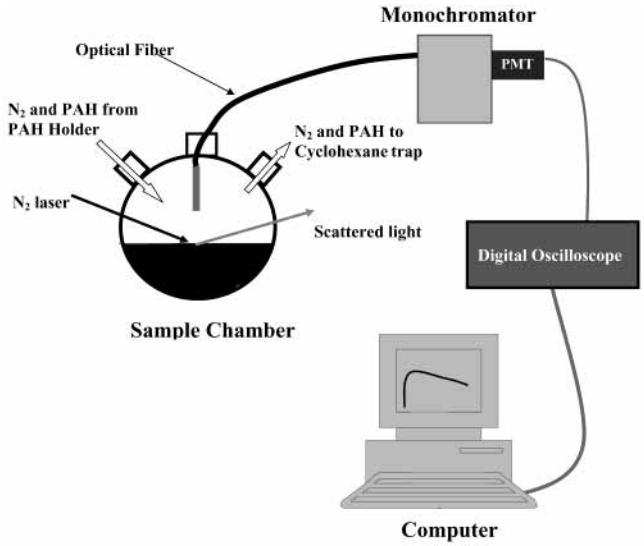

Figure 1. Schematic representation of the kinetic uptake experimental setup.

suspended 3 cm above the solution surface imaged the fluorescence into a monochromator set to a have spectral bandwidth of 4 nm. The signal was detected by a photomultiplier tube, whose output was sent to a digital oscilloscope and computer for analysis. Time-resolved signals were averaged by the oscilloscope for several seconds for each data point recorded.

The fluorescence intensity at 402 nm was recorded at a 25 ns delay time, following the laser pulse every 15 s for about 30 min, while anthracene flowed through the sample flask. For measurements of pyrene uptake, fluorescence was measured at 384 nm with a 100 ns delay as the surface was exposed to pyrene. A resolved fluorescence spectrum was acquired at the end of the ~30 min exposure period for all the PAH uptake runs. Spectra of anthracene were constructed by taking the fluorescence intensity at 25 ns delay from a series of fluorescence decay curves monitored from 350 to 500 nm, at intervals of 2 nm over the range 380−410 nm and at 5 nm intervals in the 350−380 nm and 410−500 nm ranges. In the case of pyrene, spectra were obtained from a series of fluorescence decay curves monitored at wavelengths from 350 to 500 nm, at 2 nm intervals over the range 370−395 nm, and at 5 nm intervals in the 350−370 nm and 395−500 nm ranges. Figure 2 displays the fluorescence spectra of anthracene and pyrene measured in this way, following 30 min of exposure to PAH.

Pyrene (98%), anthracene (98%), 1-octanol (99%), and hexanoic acid (99%) were purchased from Aldrich and used without further purification. Solutions were made volumetrically with distilled water and the respective solvents.

Kinetic Model of Uptake

The 3-phase (gas, surface, solution) system may be modeled as the species X (i.e. anthracene), which can exist in either of the bulk phases and can also occupy vacant surface sites, denoted Σ

$$X^g + \Sigma \underset{k_{-1}}{\overset{k_1}{\rightleftharpoons}} X^{surf} \underset{k_2}{\overset{k_{-2}}{\rightleftharpoons}} X^{aq} + \Sigma$$

where X^{surf} represents a surface-bound X molecule and the total concentration of surface sites is $[\Sigma^*] = [\Sigma] + [X^{surf}]$. We explicitly consider the processes, numbered 1 and 2, which populate the surface sites from the gas (process 1) and solution (process 2) phases, as well as the reverse, depopulation processes (−1 and −2, respectively). In this simple model, each surface

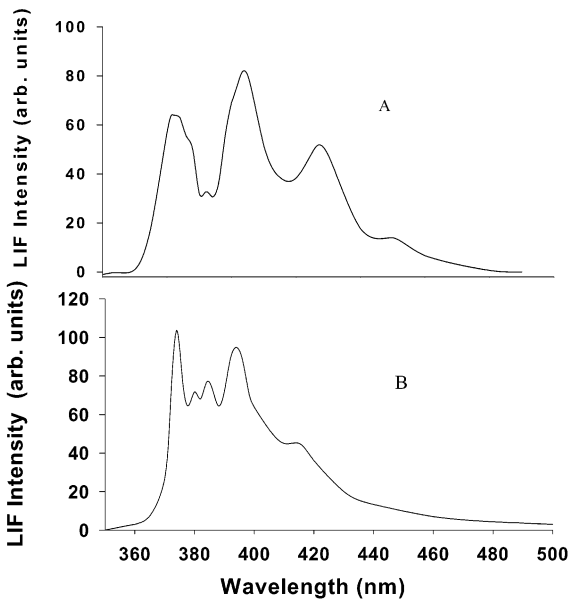

Figure 2. Emission spectra of (A) anthracene and (B) pyrene, measured at the pure air−water interfac at the end of the 30 min acquisition period of depositing the PAHs to the interface from the gas phase.

site acts independently, so adsorption takes place via a Langmuir mechanism. This gives rise to the general set of kinetic equations:

$$(d/dt)[X^g] = -k_1[X^g][\Sigma] + k_{-1}[X^{Surf}]$$

$$(d/dt)\,[X^{aq}] = -k_2[X^{aq}][\Sigma] + k_{-2}[X^{Surf}]$$

$$(d/dt)\,[X^{Surf}] = k_2[X^{aq}][\Sigma] - k_{-2}[X^{Surf}] + k_1[X^g][\Sigma] - k_{-1}[X^{Surf}] = (k_2[X^{aq}] + k_1[X^g])[\Sigma] - (k_{-2} + k_{-1})[X^{Surf}]$$

$$(d/dt)\,[\Sigma] = -\,d/dt\,[X^{Surf}]$$

In our particular experiment, the gas-phase concentration is held constant at the (we assume) room temperature vapor pressure of the PAH, so $(d/dt)\,[X^g] = 0$. Also, because the PAH solubilities in water are very low (e.g., the solubility of anthracene in water is 0.045 g m^{-3}),[22] and the experiment starts out with no PAH in solution, we ignore the transport of PAH to the interface from solution. These assumptions give rise to the simplified expression

$$(d/dt)\,[X^{Surf}] = k_1[X^g][\Sigma] - (k_{-2} + k_{-1})[X^{Surf}]$$

for the surface-bound species. Replacing $[\Sigma] = [\Sigma^*] - [X^{Surf}]$, we obtain

$$(d/dt)\,[X^{Surf}] = k_1[X^g][\Sigma^*] - (k_1[X^g] + k_{-2} + k_{-1})[X^{Surf}]$$

whose solution is

$$[X^{Surf}] = \frac{k_1[X^g][\Sigma^*]}{k_1[X^g] + k_{-1} + k_{-2}}(1 - e^{-(k_1[X^g] + k_{-1} + k_{-2})\,t}) \quad (1)$$

When the pseudo-first-order rate coefficients for loss from the surface are small compared to uptake to the surface, this expression reduces further to

$$[X^{Surf}] = [\Sigma^*]\,\{1 - \exp(-k_1[X^g]t)\} \quad (2)$$

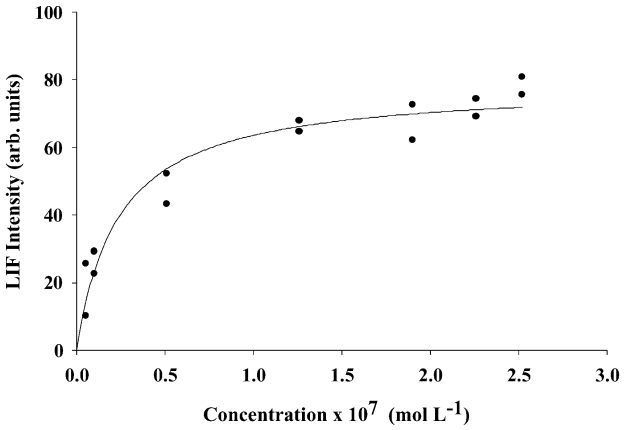

Figure 3. Fluorescence intensity from anthracene at the air−water interface as a function of its concentration in solution. The results from two separate runs are shown; the line shows a fit to a Langmuir adsorption isotherm.

In the expressions given above, the rate coefficient for surface adsorption, k_1, incorporates gas-phase diffusion, the gas−surface collision rate, geometric terms, and an uptake coefficient, γ, which gives the fraction of gas−surface collisions which result in X being bound at the interface.

If k_{-2} is significant, the species X will dissolve rapidly into solution, with some fraction (which we would observe) partitioned to the air−water interface. In this instance, the observed time dependence of X^{Surf} should reflect the kinetics of uptake into solution, rather than to the interface. The instantaneous nonreactive uptake of X into solution through a planar interface is reasonably well represented by[23]

$$\frac{1}{\gamma(t)} = \frac{1}{\alpha} + \frac{\langle c \rangle}{4RTH\sqrt{\frac{\pi t}{D_l}}} \qquad (3)$$

where α represents the mass accommodation coefficient at the surface, H gives the Henry's law constant, $\langle c \rangle$ is the average molecular speed, and D_l is the liquid-phase diffusion coefficient. For values of $H < 10^3$ mol L^{-1} atm^{-1}, the second term is expected to dominate this expression, and the uptake will decrease as $t^{-1/2}$ until equilibrium is reached. In an experiment that measures the concentration gain into the condensed phase, a square root dependence on time is expected. Uptake onto the surface may therefore be distinguished from uptake into solution by the slope of a log $[X^{surf}]$ versus log t plot: from (3), a slope of $^1/_2$ indicates uptake into solution, while uptake to the surface, as modeled by (1) and (2), yields a slope of unity.

Results

(a) Equilibrium Measurements. No evidence for exciplex formation was observed in any of the spectra measured here. Therefore, following our previous work,[17] we take the measured fluorescence intensities to be proportional to the surface concentration of PAH. Figure 3 displays the laser induced fluorescence (LIF) signal intensity as a function of the bulk concentration of anthracene in water. The results of two separate experiments are shown, as well as a fit of the data to a Langmuir adsorption isotherm. It is clear that, at least over this concentration range, the data are well represented by a Langmuir isotherm, implying that anthracene partitions readily from aqueous solution to the air−water interface, and confirming that the LIF technique employed here is sensitive to the air−water interface concentrations of PAHs. This was the conclusion of our previous study[17] as well.

To our knowledge, this is the first report of the air−water interface adsorption behavior of anthracene in aqueous solution. There is only a very small change in surface tension between pure water and a saturated solution of anthracene, making the construction of an adsorption isotherm from such measurements[1−4] impractical. Thus, we have no calibration relating the LIF signal intensity to the anthracene number density at the interface. We estimate the latter by combining gas−surface and gas−solution partition coefficients. The reported values for the Henry's law constant of anthracene in water[24] range from 1.4 to 56 mol kg^{-1} bar^{-1}. The compilation by Mackay and Shiu[25] suggests a value of 17 mol kg^{-1} bar^{-1}; this value seems most reasonable, as it lies between those reported[24] for naphthalene (~2 mol kg^{-1} bar^{-1}) and pyrene (~80 mol kg^{-1} bar^{-1}). A value of 17 mol kg^{-1} bar^{-1} is used for the purposes of the surface coverage estimate. The gas−water surface partition constant can reasonably be estimated to be 0.5 (mol m^{-2})/(mol m^{-3}) from the extrapolation presented by Pankow.[5] By use of these parameters, a bulk solution concentration of 1×10^{-7} mol L^{-1} in equilibrium with the gas and surface phases implies a surface concentration of 7.2×10^{12} molecules cm^{-2}. Using this value to calibrate the data in Figure 3, we estimate (within a factor of 2) a saturated surface coverage at equilibrium of 1×10^{13} molecules cm^{-2} for anthracene at the air−water interface. This is about 3% of the surface concentration of solid anthracene, derived from its density.

(b) Time-Dependent Measurements. Figure 4a displays the time dependence of the fluorescence intensity as anthracene is introduced to the sample chamber. The different sets of points correspond to results from solutions of different 1-octanol concentration, as noted in the caption, and the solid lines show fits to the equation

$$I = I^{max}\{1 - \exp(-k_{obs}\, t)\} \qquad (4)$$

with k_{obs} and I^{max} used as fitting parameters. Several runs at each 1-octanol concentration are shown on the plot to indicate the reproducibility of the measurements. It is clear by inspection that the uptake depends on the concentration of 1-octanol present in solution. The parameters obtained from fits of the data in Figure 4a are listed in Table 1.

Figure 4b displays log(LIF intensity) − log(time) plots for some of the data given in Figure 4a. Similar log − log plots for almost all of the PAH/organic film combinations measured here have slopes that are close to unity. This observation, and the good fits of the experimental data to (4), strongly imply that we are measuring the uptake of PAH to the air−aqueous interface in these experiments. To further test whether there was any appreciable uptake to the bulk solution phase, 3 mL aliquots of the solution were withdrawn after 1 min and after 30 min of exposure to anthracene. Fluorometric analysis of these aliquots showed them to be almost identical, with less than 10^{-8} mol L^{-1} of anthracene taken into solution during the exposure time.

To obtain an estimate of the anthracene surface concentrations displayed in Figure 4a, its uptake onto a pure water surface was measured, preceded immediately by a separate measurement of the fluorescence intensity from a saturated solution of anthracene in water. The signal level recorded for the latter measurement is equivalent to 9 units on the intensity axis in Figure 4a. Under our experimental conditions, the air−water surface achieves the same interfacial concentration of anthracene as that of a saturated solution, ~10^{13} molecules cm^{-2}, after about 30 min of exposure. Using this as a calibration, and assuming that changes in the fluorescence intensity at the interface reflect

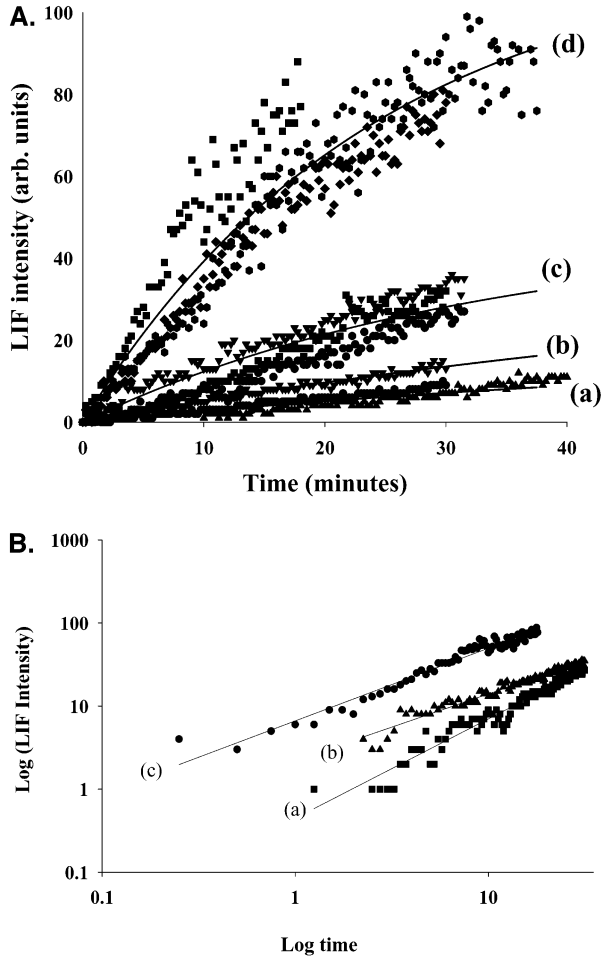

Figure 4. A. Anthracene fluorescence intensity as a function of time at (a) the pure air−water interface and at the surfaces of aqueous solutions of 1-octanol with concentrations of: (b) 1.3×10^{-3} mol L^{-1}, (c) 2.5×10^{-3} mol L^{-1}, and (d) 6.3×10^{-3} mol L^{-1}. The solid lines show fits to the data to equation 4. B. log − log plots of some of the data shown in Figure 4a. Line (a) indicates uptake onto pure water and has a slope of 1.2., line (b) corresponds to uptake onto 2.5×10^{-3} mol L^{-1} 1-octanol solution (slope = 0.80), and line (c) shows uptake onto 6.3×10^{-3} mol L^{-1} 1-octanol (slope = 0.87).

only changes in surface concentration, the results shown in figure 4a suggest that the surface concentration of anthracene in the 6.3×10^{-3} mol L^{-1} solution is about 10 times greater than that at the pure water interface.

In addition to the studies using anthracene, we performed some experiments to measure the uptake of pyrene onto water surfaces coated with either 1-octanol or hexanoic acid. Following each of these experiments, the fluorescence spectrum of pyrene at the interface was measured, as described in our previous publication.[17] A representative spectrum is shown in Figure 2. This spectrum, and in particular the relative intensities of two vibronic bands (generally labeled I and III in the literature), is quite sensitive to the polarity of pyrene's local environment. The III/I ratios measured here are given in Table 2, as well as those reported in ref 17, for comparison. Fluorescence spectra of pyrene measured at the 1-octanol-coated surface show significantly greater III/I ratios than those measured at the hexanoic-acid-coated surface, implying that the alcohol-coated interface represents a less polar environment.

Uptake parameters were obtained for pyrene in the same way as for anthracene. The derived values of k_{obs} and I^{max} are listed in Table 1. In the measurements of pyrene uptake onto hexanoic-acid-coated interfaces, the signal-to-noise ratio was quite low.

TABLE 1. Fitting Parameters[a] for Fluorescence Intensity as Function of Time for Uptake of Anthracene and Pyrene at the Air-solution Interface

conc of film-forming species (mol L^{-1})	I^{max} (arb units)	k_{obs} (10^{-2} min^{-1})	initial slope (10^{-3} s^{-1})
uptake of anthracene on 1-octanol solutions			
0	20 ± 6	1.47 ± 0.42	5.8 ± 1.5
1.3×10^{-3}	40 ± 6	1.38 ± 0.25	12.3 ± 4.1
2.5×10^{-3}	47 ± 1	3.04 ± 0.18	20.1 ± 7.0
6.3×10^{-3}	116 ± 3	4.13 ± 0.24	67 ± 18
uptake of pyrene on 1-octanol solutions			
0	23 ± 2	1.51 ± 0.19	4.3 ± 1.5
6.3×10^{-3}	76 ± 6	2.91 ± 0.30	27 ± 9
uptake of pyrene on hexanoic acid solutions			
0	23 ± 2	1.51 ± 0.19	4.8 ± 1.5
4.0×10^{-3}	31	1.6	8.8 ± 3.0
8.0×10^{-3}	46	1.4	11.4 ± 4.0
12.0×10^{-3}	50	1.3	10.2 ± 3.5

[a] Quoted errors are ± 1σ errors to the fit of the averaged data from several runs. The run-to-run reproducibility is apparent from Figure 4a.

TABLE 2. The Ratio of Fluorescence Intensity of Peak III to Peak I for Pyrene in Various Media

	III/I ratio	
	equilibrium	uptake
in pure water	0.64(±0.01)	
on the pure water surface	0.74(±0.03)[a,b]	0.77(±0.04)[c,d]
on 0.004 M hexanoic acid in water	0.88(±0.04)[a,b]	0.89(±0.05)[c,d]
on 0.008 M hexanoic acid in water	0.89(±0.04)[a,b]	0.91(±0.05)[c,d]
on 0.012 M hexanoic acid in water	0.91(±0.04)[a,b]	0.94(±0.06)[c,d]
on 0.006 M 1-octanol in water		1.46[c,d]
3.1×10^{-6}M pyrene in 1-octanol		1.66(±0.02)[c]

[a] Adapted from ref 17. [b] Measured at the air−solution interface with partitioning from the solution phase. [c] This work. [d] Measured at the air−solution interface with adsorption from the gas phase.

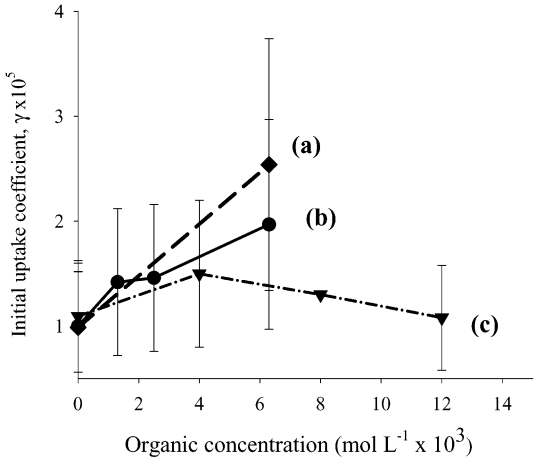

Figure 5. Surface uptake coefficients as a function of concentration of 1-octanol or hexanoic acid for (a) anthracene on 1-octanol-coated surfaces, (b) pyrene on 1-octanol-coated surfaces, and (c) pyrene on hexanoic-acid-coated surfaces. The lines are shown merely to guide the eye.

Unconstrained fits of the time dependence did not yield physically meaningful parameters. For these results only, the relative values of I^{max} were assumed to scale with hexanoic acid concentration in the same way as those we determined for equilibrium partitioning (shown in Figure 5 of our previous work[17]), and the data were fit to equation (4) with I^{max} fixed.

Discussion

All but two (out of 17) of the slopes of the log(intensity) versus log(time) plots for PAH uptake onto aqueous surfaces

measured here lie between 0.8 and 1.2. Both anthracene and pyrene have low solubilities in water and a strong propensity to partition from solution to the water surface, as suggested for anthracene by Figure 3 and shown for pyrene in our earlier work.[17] Tests of the bulk solution phase for anthracene also showed insignificant amounts of the PAH. These observations strongly imply that the uptake we measure is to the aqueous surface, rather than into the bulk solution.

The rate of adsorption of a trace gas species to the air−aqueous interface is expected to depend on many factors: its concentration in the gas and solution phases, the diffusion coefficient in air, and the probability of remaining at the interface following a collision. These are incorporated into a phenomenological uptake coefficient, which is related to the k_{obs}, measured here. To obtain the results shown in Figure 4a, only the concentration of 1-octanol differs from one experiment to another. Therefore, the differences we observe in k_{obs} must relate to differences in the adsorption probability of a PAH molecule following a collision with the liquid surface, depending upon the nature of the interface. Furthermore, the observation of these substrate-dependent differences strongly implies that gas-phase diffusion to the surface is not a limiting factor in the measured uptake kinetics.

The results presented in Figure 4a and Table 1 indicate a dependence of the uptake of both anthracene and pyrene on the solution concentration of 1-octanol. Within the uncertainties of our measurements, no such dependence is seen for the uptake of pyrene onto the surface of hexanoic acid solutions. From measurements of the adsorption of hexanoic acid[4] and 1-octanol[26] to the air−water interface, we may establish that, over the range of concentrations used here, the surface is enriched in the organic, with from about 0.1 up to a few monolayers present in each case. We did not observe any phase separation at the lower concentrations; at the highest concentrations, some octanol droplets were formed but were aspirated off the surface prior to the uptake measurement. The different uptake behavior of the 1-octanol and hexanoic-acid-coated surfaces must, therefore, be due to their different nature, rather than significant differences in the degree of surface coverage.

A clue to their different natures is found in the fluorescence spectra of pyrene measured on the two surfaces. As we discuss at some length in ref 17, on hexanoic-acid-coated surfaces, pyrene displays a III/I intensity ratio intermediate between that seen on the pure water surface and the pure hexanoic acid surface. Table 2 illustrates that we obtain the same result following an uptake experiment as that obtained for the equilibrium system. By contrast, the III/I ratio seen for pyrene following uptake onto a 1-octanol-coated surface is very different, close to that observed in 1-octanol solution. This significantly larger III/I ratio is indicative of a less polar environment for pyrene at the 1-octanol-coated surface than that at the hexanoic-acid-coated surface. We propose that the longer hydrocarbon chain and lower solubility of 1-octanol in water gives rise to a more hydrophobic interface. This, in turn, is likely to be considerably better at solvating the hydrophobic pyrene at the surface than is the less hydrophobic hexanoic-acid-coated interface. The enhanced solubility might explain why the uptake rate is larger for pyrene on the 1-octanol-coated surface than on the acid-coated surface.

Recent work by Nathanson and co-workers[27] has also indicated a dependence of uptake probabilities on the nature and composition of the interface. Studies of the kinetic energy distributions of molecular beams of HX molecules scattered from an aqueous D_2SO_4 surface showed that the fraction of scattered HX molecules which had undergone isotopic exchange were seen to increase as the acid concentration was lowered. The surface of sulfuric acid solutions is believed to be composed primarily of neutral acid and water molecules.[28,29] Because water is a stronger base than sulfuric acid, surface hydrogen bonding, which leads to trapping and isotope exchange, is expected to depend on the surface water concentration. The molecular beam scattering results were interpreted as indicating a greater surface trapping (and subsequent isotopic exchange) probability with increasing acid dilution, as the acid surface became richer in neutral water.

The results presented in Table 1 indicate a dependence of the uptake parameters on the concentration and the nature of any organic surface film present. With a few assumptions, we can use the kinetic model presented above to estimate the uptake coefficients to the different surfaces. The kinetic model suggests that the parameter k_{obs} should be related to the rate coefficients for adsorption and desorption

$$k_{obs} = k_1[X^g] + k_{-1} + k_{-2}$$

In principle, all three of the rate coefficients could depend on the surface concentration of organic. We have argued above that the present experiment measures uptake to the surface alone; this implies that k_{-2} is small with respect to the other parameters. It will be ignored in what follows. As well, we assume that gas phase diffusion is sufficiently rapid that it does not contribute to k_{obs}.

The contributions of the surface uptake, $k_1[X^g]$, and the surface evaporation, k_{-1} terms to k_{obs} may be estimated as follows:

Assuming gas-phase anthracene to be present at its room temperature vapor pressure of 8×10^{-4} Pa,[30] its collision rate with the surface is 5×10^{14} molecules cm^{-2} s^{-1}. Combined with our estimate of 10^{13} molecules cm^{-2} for the total number of available surface sites at the air-pure water interrface, this collision rate yields a collision frequency of gas-phase molecules with surface sites of about 50 s^{-1}. The rate coefficient for evaporation from the surface, k_{-1}, may be estimated from transition state theory as

$$k_{-1} = \frac{k_B T}{h} e^{(-\Delta G^{\#}/k_B T)} \qquad (5)$$

where k_B and h represent Boltzmann's and Planck's constants respectively, and $\Delta G^{\#}$ represents the free energy of activation for evaporation. As a lower limit, this parameter is given by the free energy of adsorption, which may be estimated from data given in refs 5 and 9 to be at least 50 kJ mol^{-1} for anthracene. The upper limit for the evaporation rate coefficient is thus 1.1×10^4 s^{-1}. When there is a free energy barrier to evaporation in excess of the adsorption free energy, which must be the case when the uptake coefficient is significantly less than unity, the evaporation rate coefficient will be less than this. However, the reduction in the evaporation rate coefficient will be matched by a reduction in the uptake coefficient, so the relative importance of uptake to evaporation is not influenced. We conclude that $k_1[X^\gamma]$ is probably less than k_{-1}, so that γ cannot be related directly to k_{obs}.

At early times, however, the rate of surface population (the uptake rate) will be larger than the evaporation rate, because the surface will be sparsely populated. At short times (2) gives a linear increase of concentration with time

$$(d[X^{Surf}]/dt) = k\gamma[X^\gamma][\Sigma^*] \qquad (6)$$

where g is now explicitly included. By use of our calibration for the fluorescence intensity, which sets $[\Sigma^*] = 10^{13}$ molecules cm^{-2} for the pure water surface, the initial slopes in Figure 4a

may be related to the rate of surface coverage increase, from (6). These initial slopes are reported in Table 1 for all the solutions measured here. Through this procedure, a value of $(5 \pm 3) \times 10^9$ molecules cm^{-2} s^{-1} is obtained for the initial rate of anthracene uptake to the air−water interface. The 60% error estimate incorporates the uncertainties in the saturated surface coverage and in the measurement of the initial slopes.

Dividing the initial surface uptake rate by the surface collision rate yields surface uptake coefficients, shown as a function of solution composition in Figure 5. The error bars in the Figure reflect the uncertainties given above for the initial uptake rates and do not include any estimate of the uncertainty in the partial pressure of anthracene above the sample solution, because we have no way of ascertaining this. Assuming similar saturated coverages for pyrene and anthracene on the pure water surface, we may obtain uptake coefficients for pyrene as well. For both anthracene and pyrene, a value of $\gamma = 1 \times 10^{-5}$ (to one significant figure) is obtained for the air−pure-water interface. To obtain uptake coefficients for the organic-coated surfaces, we require the corresponding values of the saturated surface coverage of PAH, [Σ*], appearing in (6). Our experiments provide no direct measurement of this quantity. However, as long as the LIF intensity remains directly proportional to the surface concentration of PAH, it is reasonable to assume that [Σ*] scales linearly with the values of I^{max}, shown in Table 1. We derive the uptake coefficients of both anthracene and pyrene using this scaling. These are shown in Figure 5. They increase monotonically with the concentration of 1-octanol in solution over the range explored here. The presence of hexanoic acid at the interface has no significant effect on the uptake rate of pyrene from the gas phase.

The surface uptake coefficients derived here are the 2-D analogues of those for uptake into solution, in the absence of reaction; they indicate the fraction of collisions that a gas-phase molecule makes with the surface that result in its loss from the gas phase. Of course, just as for uptake leading to bulk solvation, molecules at the surface are exchanging with their gas-phase counterparts at all times; at equilibrium (or at any rate, at steady state) the rates of surface population (through uptake) and depopulation (through evaporation) are equal. The time dependence of the surface concentrations of the PAH compounds studied here, shown in Figure 4a, indicate an approach to such a steady state at longer times.

An uptake coefficient of about 10^{-5} for anthracene or pyrene onto the water surface is considerably smaller than those reported for uptake of small alcohols, acids and aldehydes by water, which are generally several orders of magnitude larger.[31,32] Although those compounds are all considerably more soluble than the PAHs studied here, and thus their uptake coefficients reflect uptake into solution, rather than to the surface, at least for some there is thought to be a significant component of surface adsorption contributing to the measured uptake. As noted above, strong attractive interactions between solution molecules present at the surface of a liquid and incoming gas phase molecules can increase the uptake. It is, therefore, not surprising that PAH uptake to the pure water surface is much smaller than the surface component of the uptake of aldehydes to the same surface. The increasingly hydrophobic nature of the interface as the 1-octanol solution concentration increases, indicated by the pyrene III/I ratios, presumably increases the trapping ability of the surface toward anthracene and pyrene.

Conclusions

In this work, we used a glancing angle laser-induced fluorescence technique to monitor uptake kinetics of anthracene and pyrene from the gas phase to the air−aqueous interface in the presence and absence of an organic coating. There is enhanced uptake of both compounds to the air−solution interface when the interface is coated with 1-octanol; this seems not to occur when the surface has a hexanoic acid film. Analysis of the III/I fluorescence intensity ratios in the pyrene spectra indicate that 1-octanol-coated surfaces present a more hydrophobic environment than hexanoic-acid-coated surfaces. An estimate of the uptake coefficients to the interface gives $\gamma = 1 \times 10^{-5}$ for the pure air−water interface, with a monotonic increase with increasing solution concentration of 1-octanol, to about $(2-3) \times 10^{-5}$ for the fully coated aqueous surface.

Acknowledgment. We are grateful to Jonathan Abbatt for helpful discussions of these results. This work was funded by CFCAS and NSERC. B.T.M. thanks the University of Botswana for a Staff Development Program scholarship.

References and Notes

(1) Donaldson, D. J. *J. Phys. Chem. A* **1999**, *103*, 62.
(2) Donaldson, D. J.; Anderson, D. *J. Phys. Chem. A* **1999**, *103*, 871.
(3) Mmereki, B. T.; Donaldson, D. J.; Hicks, J. M. *J. Phys. Chem. A* **2000**, *104*, 10789.
(4) Demou, E.; Donaldson, D. J. *J. Phys. Chem. A* **2002**, *106*, 982.
(5) Pankow, J. F. *Atmos. Environ.* **1997**, *31*, 927.
(6) Gustafsson, O.; Gschwend, P. M. *Atmos. Environ.* **1999**, *33*, 163.
(7) Hoff, J. T.; Mackay, D.; Gillham, R.; Shiu, W. Y. *Environ. Sci. Technol.* **1993**, *27*, 2174.
(8) Bruant, R. G., Jr.; Conklin, M. H. *J. Phys. Chem. B* **2002**, *106*, 2224.
(9) Raja, S.; Yaccone, F. S.; Ravikrishna, R.; Valsaraj, K. *J. Chem. Eng. Data* **2002**, *47*, 1213
(10) Roth, C. M.; Goss, K.-U.; Schwarzenbach, R. P. *J. Colloid Interface Sci.* **2002**, *252*, 21.
(11) Gill, P. S.; Graedel, T. E. *Rev. Geophys.* **1983**, *21*, 903.
(12) Tervahattu, H.; Juhanoja, J.; Kupiainen, K. *J. Geophys. Res. D* **2002**, *107*, D. O. I. 10.1029/2001JD001403.
(13) Ellison, G. B.; Tuck, A. F.; Vaida, V. J. *Geophys. Res.* **1999**, *104*, 11633.
(14) Wadia, Y.; Finlayson-Pitts, B. J.; Tobias, D. J.; Stafford, R. *Langmuir* **2000**, *16*, 9321.
(15) Lo, J. H. A.; Lee, W. M. G. *Chemosphere* **1996**, *33*, 1391.
(16) Huang, H. L.; Lee, W. M. G. *J. Environ. Eng.* **2002**, *128*, 60.
(17) Mmereki, B. T.; Donaldson, D. J. *Phys. Chem. Chem. Phys.* **2002**, *4*, 4186.
(18) (a) Glotfelty, D. E.; Seiber, J.N; Lilje, L. A *Nature*, **1986**, *325*, 602. (b) Glotfelty, D. E; Majewski, M. S; Seiber, J. N *Environ. Sci. Technol.* **1990**, *24*, 353.
(19) Capel, P. D; Leuenberger, C.; Giger, W. *Atmos. Environ.* **1991**, *25A*, 1335.
(20) Schomburg, C. J.; Glotfelty, D. E.; Seiber, J. N. *Environ. Sci. Tech.* **1990**, *25*, 155.
(21) Sagebiel, J. C.; Seiber, J. N. *Environ. Tox. Chem.* **1993**, *12*, 813.
(22) Shiu, W.-Y.; Ma, K.-C. *J. Phys. Chem. Ref. Data*. **2000**, *29* (1), 41.
(23) Shi, Q.; Li, Y. Q.; Davidovits, P.; Jayne, J. T.; Worsnop, D. R.; Mozurkewich, M.; Kolb, C. E. *J. Phys. Chem. B* **1999**, *103*, 2417.
(24) NIST Standard Reference Database Number 69-February 2000 release; http://webbook.nist.gov/chemistry/.
(25) 25.Mackay, D.; Shiu, W. Y. *J. Phys. Chem. Ref. Data* **1981**, *10*, 1175.
(26) Lin, S.-Y.; Wang, W.-J.; Hsu, C.-T. *Langmuir* **1997**, *13*, 6211.
(27) Behr, P.; Morris, J. R.; Antman, M. D.; Ringeisen, B. R.; Splan, J. R.; Nathanson, G. M. *Geophys. Res. Lett.* **2001**, *28*, 1961.
(28) Raduge, C.; Pflumio, V.; Shen, Y. R. *Chem. Phys. Lett.* **1997**, *274*, 140.
(29) Schnitzer, C.; Baldelli, S.; Shultz, M. J. *Chem. Phys. Lett.* **1999**, *313*, 416.
(30) Finlayson-Pitts, B. J.; Pitts, J. N., Jr. *Chemistry of the Upper and Lower Atmosphere*;Academic Press: New York, 2000.
(31) Jayne, J. T.; Duan, S. X.; Davidovits, P.; Worsnop, D. R.; Zahniser, M. S.; Kolb, C. E. *J. Phys. Chem.* **1992**, *96*, 5452.
(32) Jayne, J. T.; Duan, S. X.; Davidovits, P.; Worsnop, D. R.; Zahniser, M. S.; Kolb, C. E. *J. Phys. Chem.* **1991**, *95*, 6329.